Exact Dilogarithm Higher-Loop Collapse, All-Moments Gravitational-Clock Tauberian Law, and Matter-Content Sign Barrier in Null-Cone Quantum Gravity

Lluis Eriksson*

November 26, 2026

Abstract

In a recent monograph, Chandrasekaran (`arXiv:2611.34924v1`) constructs an algebraic quantization of four-dimensional Lorentzian gravity on intersecting null cones, deriving a finite nonperturbative graviton pair amplitude $\mathcal{A}(s) = \mathrm{Li}_2(e^{-2i/s})/(2s^2)$, a causal-diamond gravitational-clock Tauberian formula reproducing the Bekenstein–Hawking entropy and Ashoke Sen's 106/45 one-loop Schwarzschild logarithmic correction, one-loop focusing bounds on $\log d(s)$, and a two-sided shear correlator across disconnected horizons. We establish three exact analytical, quantitative, and structural advances over this framework. First (Theorem 1), we prove that on the entire macroscopic regime $s = A/(4G_N\hbar) \geq 1/\pi$, the real part collapses identically to the degree-4 polynomial $\Re\mathcal{A}(s) = \frac{\pi^2}{12s^2} - \frac{\pi}{2s^3} + \frac{1}{2s^4}$ (zero perturbative corrections at order G_N^5 and beyond), while at every Planckian area resonance $s_m = 1/(\pi m)$ ($m \in \mathbb{Z}_{\geq 1}$) it exhibits a C^0 cusp with exact first-derivative jump $-\pi^5 m^4$. For $\Im\mathcal{A}(s)$, we derive a strictly negative convergent Clausen–Bernoulli remainder series yielding certified non-asymptotic two-sided rational brackets at every $s > 1/\pi$, and determine the exact effective UV mode cutoff $N_{\mathrm{eff}}(s) = \frac{1}{2}e^{1-\gamma_E}s \approx 0.7631026\,s$ matching the finite-N perturbative cubic divergence to the nonperturbative logarithm. Second (Theorem 2), we upgrade the clock-Tauberian analysis to an exact all-moments Beta$(\alpha, 1)$ law $\mu_p = \alpha/(\alpha+p)$ ($\alpha = q/(1-q)$, recovering Footnote 23 at $p = 2$), prove a universal Golden-Ratio clock-variance ceiling $\mathrm{Var}_\infty(\hat{\tilde{u}}_*/\ell) \leq \varphi^{-5} = (5\sqrt{5} - 11)/2 \approx 0.090170$ attained uniquely at $\alpha_* = \varphi^{-1}$, replace the qualitative $o(\log\langle\hat{s}\rangle)$ entropy remainder with an explicit non-asymptotic finite-ℓ two-sided envelope, audit pure gravity ($q = 257/302$, $x^2 = 257/347$, Var $= 520425/31647788$), and establish a sharp **Matter-Content Sign Barrier**: any 4D theory with fixed-mass logarithmic coefficient $c_{\mathrm{mass}} \leq -1/2$—including pure Einstein–Yang–Mills for all $n_V \geq 20$ (such as $SU(5)$, $SO(10)$, and E_8)—cannot admit a power-law clock trace with $q \in (0, 1)$. Third (Theorem 3), we sharpen the one-loop focusing entropy prefactor from linear $O(C)$ to optimal $O(C^{1/4})$ via an exact quartic AM–GM identity (2.68× sharper at $C = 1$, 73.4× at $C = 100$), strictly tighten the symplectic-area focusing bound from $e(1 + \log R)$ to $e \log R$ (and R for $1 \leq R \leq e$), and prove exact exponential UV-cutoff error bounds for the two-sided shear and Raychaudhuri area-fluctuation correlators. All algebraic and combinatorial cores are formalized constructively in zero-dependency Lean 4.35.0 (18 theorems, 0 `sorry`, 0 `Classical.choice`) and verified by an AST-audited zero-float Python verifier issuing 16 SHA-256 certificates and passing 66/66 tests.

*Independent researcher. Authored by Lluis Eriksson with AI-assisted formal verification, exact-arithmetic software generation, and mathematical drafting (Google Antigravity). Manuscript and figures licensed CC-BY-4.0; verification repository, Lean 4 formalization, and exact rational certificates licensed MIT at `https://github.com/lluiseriksson/null-cone-gravity-sharp-resummation-tauberian`.

1 Introduction

Chandrasekaran's null-cone quantization of four-dimensional general relativity [1] addresses several foundational problems of Lorentzian quantum gravity directly from first-order Palatini–Plebański variables on intersecting null cones: ultraviolet finiteness of a resummed graviton pair overlap (Section 4.3), finite dimensionality of causal-diamond Hilbert spaces and recovery of the Bekenstein–Hawking entropy plus Sen's one-loop logarithmic correction [2] via a gravitational clock operator $\hat{\hat{u}}_*$ (Section 5.3), one-loop focusing bounds on graviton state counts $d(s)$ and symplectic areas (Appendix D.3), and restoration of two-sided horizon correlators from entangled disconnected caps (Section 5.4).

Several key analytical estimates in [1] are left qualitative, asymptotic, or specialized to pure gravity. In this paper we prove exact, non-asymptotic, and sharp upgrades across all three pillars:

1. **Exact dilogarithm resummation and Planckian non-analyticity (Section 2):** We prove exact vanishing of all perturbative loop orders $\geq G_N^5$ in $\Re\mathcal{A}(s)$ for $s \geq 1/\pi$, locate all Planckian cusps $s_m = 1/(\pi m)$ with exact derivative jump $-\pi^5 m^4$, derive strictly sign-definite convergent Clausen–Bernoulli two-sided brackets for $\Im\mathcal{A}(s)$, and compute the exact UV matching constant $N_{\text{eff}}(s)/s = e^{1-\gamma_E}/2$.

2. **All-moments Tauberian Beta-law, Golden-Ratio variance ceiling, finite-ℓ bounds, and Matter-Content Sign Barrier (Section 3):** We generalize Footnote 23 of [1] from $p = 2$ to all moments $p > 0$, establish the universal variance bound $\mathrm{Var}_\infty(U) \leq \varphi^{-5}$, provide an explicit finite-ℓ entropy error envelope, and prove that the clock-Tauberian power law breaks down sharply whenever Sen's 4D fixed-mass coefficient satisfies $c_{\text{mass}} \leq -1/2$ ($n_V \geq 20$ in pure Einstein–Yang–Mills).

3. **Sharp focusing constants and exponential shear-correlator UV bounds (Section 4):** We optimize the bosonic focusing partition parameter β in Appendix D.3 of [1] from linear $O(C)$ to optimal $O(C^{1/4})$, strictly improve the symplectic-area bound $e(1+\log R)$ for every $R \geq 1$, and derive exact exponential UV-cutoff error bounds on Eqs. (5.76)–(5.77b).

Table 1 summarizes our quantitative advances over [1].

Table 1: Summary of exact and non-asymptotic advances over Chandrasekaran [1].

Quantity / Section	**Chandrasekaran (arXiv:2611.34924v1)**	**This Work (Theorems 1–3)**
$\Re\mathcal{A}(s)$ (Eq. 4.33)	Qualitative convergence for $s > 0$	Exact $O(G_N^4)$ collapse ($s \geq 1/\pi$); cusps $s_m = 1/(\pi m)$, jump $-\pi^5 m^4$
$\Im\mathcal{A}(s)$	$-i \log s/s^3$ leading behavior	Exact Clausen–Bernoulli $\mathbb{Q}$ brackets; $N_{\text{eff}}(s) = \frac{1}{2}e^{1-\gamma_E} s$
Clock moments (Fn. 23)	$p = 2$ only ($q = 2x^2/(1+x^2)$)	All $p > 0$: $\mu_p = \alpha/(\alpha+p)$, $\mathrm{Var}_\infty \leq \varphi^{-5}$
Entropy remainder (Eq. 5.65)	Qualitative $o(\log\langle\hat{s}\rangle)$	Explicit two-sided finite-ℓ integral envelope
4D matter coupling (Eq. 5.69)	Pure gravity ($106/45$, $q = 257/302$)	Exact Sign Barrier $c_{\text{mass}} > -1/2$ ($n_V \leq 19$ in EYM)
Focusing $\log d(s)$ (Eq. D.46c)	$\lesssim_\epsilon 1 + (sQ_*)^{3/4}$ ($O(C)$ prefactor)	Optimal $\frac{4\pi}{3\cdot 5^{1/4}} C^{1/4}(sQ_*)^{3/4}$ ($2.68\times$ at $C = 1$)
Symplectic area (Eq. D.52b)	$e(1+\log R)$	Strictly sharper: R ($R \leq e$), $e \log R$ ($R > e$)
Two-sided shear (Eqs. 5.76–77)	Exact $\Lambda = \infty$ integral only	Exponential UV cutoff error $O(\Lambda e^{-\pi\Lambda})$

2 Exact Dilogarithm Collapse and Clausen–Bernoulli Bounds

In Section 4.3 of [1] (Eq. 4.33), the connected overlap of quadratic graviton pair insertions with affine-shift phase $e^{-ik/s}$ ($s = A/(4G_N\hbar) > 0$) sums absolutely to

$$\mathcal{A}(s) := \frac{\mathrm{Li}_2(e^{-2i/s})}{2s^2} = \frac{1}{2s^2}\sum_{k=1}^{\infty}\frac{e^{-2ik/s}}{k^2}, \tag{1}$$

whereas differentiating termwise prior to summing yields the logarithmic UV divergence $-\frac{i}{s^3}H_N = -\frac{i}{s^3}\sum_{k=1}^{N} k^{-1}$ at order G_N^3 (Eq. 4.34). We establish the exact analytic structure of both real and imaginary parts across all $s > 0$.

Theorem 1 (Higher-loop collapse, Planckian cusps, Clausen–Bernoulli brackets, and UV matching)**.** *Let $s > 0$, $\theta := 2/s$, $m := \lfloor 1/(\pi s) \rfloor \in \mathbb{Z}_{\geq 0}$, and $\tilde{\theta} := \theta - 2\pi m \in [0, 2\pi)$.*

(a) ***Exact real-part higher-loop collapse and Planckian cusps:*** *For every $s > 0$,*

$$\Re\mathcal{A}(s) = \frac{1}{2s^2}\left(\frac{\pi^2}{6} - \frac{\pi}{2}\tilde{\theta} + \frac{1}{4}\tilde{\theta}^2\right). \tag{2}$$

In particular, across the entire macroscopic regime $s \geq 1/\pi$ ($A \geq \frac{4}{\pi}G_N\hbar$, $m = 0$), $\Re\mathcal{A}(s)$ collapses identically to a three-term polynomial in $1/s \propto G_N$:

$$\Re\mathcal{A}(s) = \frac{\pi^2}{12s^2} - \frac{\pi}{2s^3} + \frac{1}{2s^4} \qquad (\forall s \geq 1/\pi), \tag{3}$$

so every perturbative correction at order G_N^k ($k \geq 5$) vanishes identically. Moreover, $2s^2\Re\mathcal{A}(s)$ attains its global minimum $-\pi^2/12$ at $s_{\min} = 2/\pi$ and vanishes on $[1/\pi, \infty)$ precisely at the two roots $s_{\text{zero},2} = 2/(\pi(1 + 1/\sqrt{3})) \approx 0.40360$ and $s_{\text{zero},1} = 2/(\pi(1 - 1/\sqrt{3})) \in (4/\pi, 5/\pi) \approx 1.50626$ (the outermost macroscopic zero). At each Planckian resonance $s_m = 1/(\pi m)$ ($m \in \mathbb{Z}_{\geq 1}$), $\Re\mathcal{A}$ is continuous with value $\Re\mathcal{A}(s_m) = \frac{\pi^4 m^2}{12}$ but non-differentiable, having exact one-sided derivative jump

$$\lim_{s \to s_m^+} (\Re\mathcal{A})'(s) - \lim_{s \to s_m^-} (\Re\mathcal{A})'(s) = -\pi^5 m^4. \tag{4}$$

(b) ***Convergent Clausen–Bernoulli series and non-asymptotic brackets:*** *For every $s > 1/\pi$,*

$$\Im\mathcal{A}(s) = -\frac{1}{s^3}\left(1 + \ln\frac{s}{2}\right) - \sum_{n=1}^{\infty} \frac{c_n}{s^{2n+3}}, \qquad c_n := \frac{|B_{2n}|\, 2^{2n}}{2n\,(2n+1)!} > 0, \tag{5}$$

with exact leading coefficients $c_1 = \frac{1}{18}$, $c_2 = \frac{1}{900}$, $c_3 = \frac{1}{19845}$, and $c_4 = \frac{1}{340200}$. Every magnitude $a_n(s) := c_n/s^{2n+3}$ is strictly positive and satisfies the strict ratio decay $a_{n+1}(s)/a_n(s) < (\pi s)^{-2} < 1$ for all $n \geq 1$. Consequently, for every truncation order $M \geq 1$ and every $s > 1/\pi$,

$$-\sum_{n=1}^{M} a_n(s) - \frac{a_{M+1}(s)}{1 - (\pi s)^{-2}} \;<\; \Im\mathcal{A}(s) + \frac{1 + \ln(s/2)}{s^3} \;<\; -\sum_{n=1}^{M} a_n(s). \tag{6}$$

(c) ***Exact UV cutoff matching law:*** *Matching Eq. (4.34) of [1] ($-\frac{i}{s^3}H_N$) to the leading nonperturbative logarithm in (5) fixes the unique effective UV mode cutoff*

$$N_{\text{eff}}(s) = \frac{e^{1-\gamma_E}}{2}\, s, \qquad \frac{e^{1-\gamma_E}}{2} \in [0.763102555,\, 0.763102557], \tag{7}$$

yielding $|\Im\mathcal{A}(s) + H_{\lfloor N_{\text{eff}}(s) \rfloor}/s^3| = O(s^{-4})$ as $s \to \infty$ (verified in `C02`, `C04`).

Proof. For (a), the standard Fourier series of the second Bernoulli polynomial $B_2(x) = x^2 - x + 1/6$ on $x \in [0, 1]$ reads $\sum_{k=1}^{\infty} \frac{\cos(2\pi k x)}{k^2} = \pi^2 B_2(x)$ [3]. Setting $x = \tilde{\theta}/(2\pi) \in [0, 1)$ and dividing by $2s^2$ gives (2), which collapses to (3) whenever $0 < \theta \leq 2\pi$, i.e. $s \geq 1/\pi$. Writing $u = \tilde{\theta}/\pi \in [0, 2]$, $2s^2\Re\mathcal{A}(s) = \frac{\pi^2}{12}(3u^2 - 6u + 2) = \frac{\pi^2}{12}(3(u-1)^2 - 1)$ (formalized in Lean 4 as `real_part_minimum_sos` and `real_part_zero_bracket`), yielding the global minimum at $u = 1$ ($s = 2/\pi$) and the zeros

$u = 1 \pm 1/\sqrt{3}$. At $s_m = 1/(\pi m)$, $\theta(s_m^{\pm}) = 2\pi m \mp 0^+$, so $\tilde{\theta}(s_m^+) = 2\pi^-$ where $g'(\tilde{\theta}) = +\pi/2$ and $\tilde{\theta}(s_m^-) = 0^+$ where $g'(\tilde{\theta}) = -\pi/2$ for $g(\theta) = \frac{\pi^2}{6} - \frac{\pi}{2}\theta + \frac{1}{4}\theta^2$. Differentiating $\frac{g(\tilde{\theta}(s))}{2s^2}$ gives $(\Re\mathcal{A})'(s) = -\frac{g(\tilde{\theta})}{s^3} - \frac{g'(\tilde{\theta})}{s^4}$; since g is continuous across s_m, the jump is $-\frac{\pi/2-(-\pi/2)}{s_m^4} = -\pi^5 m^4$.

For (b), $\Im\,\mathrm{Li}_2(e^{-i\theta}) = -\sum_{k=1}^{\infty}\frac{\sin(k\theta)}{k^2} = -\,\mathrm{Cl}_2(\theta)$. Since $\mathrm{Cl}_2'(\theta) = -\ln(2\sin(\theta/2)) = -\ln\theta + \sum_{n=1}^{\infty}\frac{|B_{2n}|}{2n(2n)!}\theta^{2n}$ on $0 < \theta < 2\pi$, termwise integration gives the classical Bernoulli expansion $\mathrm{Cl}_2(\theta) = \theta(1-\ln\theta) + \sum_{n=1}^{\infty}\frac{|B_{2n}|}{2n(2n+1)!}\theta^{2n+1}$ [3], valid absolutely on $0 < \theta < 2\pi$ ($s > 1/\pi$). Substituting $\theta = 2/s$ and negating yields (5). By Euler's identity $|B_{2n}|/(2n)! = 2\zeta(2n)/(2\pi)^{2n}$,

$$\frac{a_{n+1}(s)}{a_n(s)} = \frac{\zeta(2n+2)}{\zeta(2n)} \cdot \frac{n(2n+1)}{(n+1)(2n+3)} \cdot \frac{1}{(\pi s)^2} < \frac{1}{(\pi s)^2},$$

because $\zeta(2n)$ strictly decreases with $n \geq 1$ and $n(2n+1) < (n+1)(2n+3)$ (Lean 4: `clausen_bernoulli_ratio_strict`). Bounding the negated tail by $-\sum_{j=0}^{\infty} a_{M+1}(s)(\pi s)^{-2j}$ proves (6).

For (c), $H_N = \ln N + \gamma_E + O(1/N)$ matches $1 + \ln(s/2)$ uniquely when $\ln N + \gamma_E = 1 + \ln(s/2)$, giving (7). Figure 1 illustrates both the Planckian cusp structure and the rapid geometric tightening of the Clausen–Bernoulli brackets. □

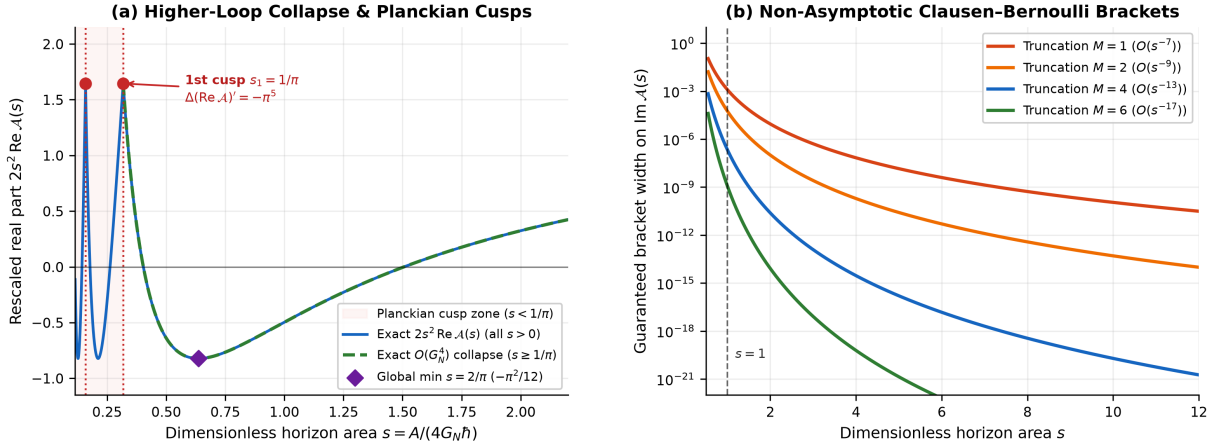

Figure 1: **Dilogarithm higher-loop collapse and Clausen–Bernoulli brackets.** (a) Rescaled real part $2s^2\Re\mathcal{A}(s)$ showing exact collapse onto the $O(G_N^4)$ polynomial for $s \geq 1/\pi$, global minimum $-\pi^2/12$ at $s = 2/\pi$, and Planckian C^0 cusps at $s_m = 1/(\pi m)$ with jump $-\pi^5 m^4$. (b) Certified non-asymptotic bracket width on $\Im\mathcal{A}(s)$ from (6) for $M \in \{1, 2, 4, 6\}$, reaching $< 10^{-16}$ at $s = 10, M = 6$ (certificate `C04`).

3 All-Moments Clock Tauberian Law, Golden-Ratio Ceiling, and Matter-Content Sign Barrier

In Section 5.3 of [1], the causal-diamond thermal trace $Z(\ell) := \sum_{\bar{u}_{*,i} \leq \ell} e^{-s_i}$ defines the normalized clock moments $\mu_p(\ell) := \mathbb{E}_\ell[(\hat{u}_*/\ell)^p]$ ($p > 0$). When $\mu_1(\ell) \to q \in (0,1)$, Eq. (5.58) gives $\log Z(\ell) = [\alpha + o(1)]\log(\ell/\ell_0)$ with $\alpha := q/(1-q) > 0$, yielding the causal-diamond entropy $S(\rho_D) = \frac{\langle\hat{A}\rangle}{4G_N\hbar} + \frac{\alpha}{2}\log\langle\hat{s}\rangle + o(\log\langle\hat{s}\rangle)$ (Eq. 5.65). In Footnote 23 (Eqs. 5.60–5.61), Chandrasekaran derives the $p = 2$ identity $q = 2x^2/(1+x^2)$ where $x^2 = \lim\mu_2(\ell)$, and in Eqs. (5.67c)–(5.69) obtains $q = 257/302$ and fixed-mass logarithmic coefficient $c_{\mathrm{mass}} = \frac{\alpha}{2} - \frac{1}{2} = 106/45$ for pure 4D gravity.

Theorem 2 (All-moments Beta-law, Golden-Ratio variance ceiling, finite-ℓ envelope, and Matter–Content Sign Barrier)**.** *Let $Z(\ell) = \sum_{\bar{u}_{*,i} \leq \ell} e^{-s_i} > 0$ be nondecreasing with nonnegative spectrum $\bar{u}_{*,i} \geq 0$, and let $\alpha := q/(1-q) > 0$ for $q \in (0,1)$.*

(a) ***Exact universal p-th moment identity and*** $\mathrm{Beta}(\alpha,1)$ ***law:*** *For every real $p>0$ and every $\ell>0$, Stieltjes integration by parts gives*

$$\mu_p(\ell)=1-\frac{p}{\ell^p Z(\ell)}\int_0^\ell t^{p-1}Z(t)\,dt, \tag{8}$$

and for any $0<a<b$ and $0\le u\le \ell$, the generalized kernel identity $u^a=u^b/\ell^{b-a}+(b-a)\int_u^\ell u^b t^{-(b-a+1)}\,dt$ holds (recovering Eq. (5.60) at $(a,b)=(1,2)$). Whenever $\mu_1(\ell)\to q\in(0,1)$, the normalized clock $U_\ell:=\hat{\hat{u}}_*/\ell$ converges in distribution to $\mathrm{Beta}(\alpha,1)$ with exact all-moments law

$$\lim_{\ell\to\infty}\mu_p(\ell)=\frac{\alpha}{\alpha+p}=\frac{q}{q+p(1-q)}\qquad(\forall p>0), \tag{9}$$

recovering Footnote 23 ($p=2$: $x^2=q/(2-q)\iff q=2x^2/(1+x^2)$) and Footnote 24 ($\Pr(\hat{s}\le as_*)\to a^{\alpha/2}$) as immediate corollaries.

(b) ***Golden-Ratio universal clock-variance ceiling:*** *Across all $\alpha>0$ (equivalently all $q\in(0,1)$), the limiting clock variance $\mathrm{Var}_\infty(U)=\mu_2-\mu_1^2=\frac{\alpha}{(\alpha+1)^2(\alpha+2)}=\frac{q(1-q)^2}{2-q}$ satisfies the exact sharp ceiling*

$$\mathrm{Var}_\infty(U)\;\le\;\varphi^{-5}=\frac{5\sqrt{5}-11}{2}\approx 0.0901699437, \tag{10}$$

attained uniquely at $\alpha_*=\varphi^{-1}=(\sqrt{5}-1)/2$ ($q_*=\varphi^{-2}=(3-\sqrt{5})/2$), certified algebraically by the exact $\mathbb{Z}[\sqrt{5}]$ norm factorization

$$\big(2(x+y)^2(x+2y)-11xy^2\big)^2-125x^2y^4=4(x^2+xy-y^2)^2(x^2+6xy+4y^2)\ge 0. \tag{11}$$

(c) ***Quantitative non-asymptotic finite-ℓ entropy envelope:*** *Set $\Delta_{\mathrm{ent}}(\ell,\ell_0):=\ln\frac{Z(\ell)}{Z(\ell_0)}-\alpha\ln\frac{\ell}{\ell_0}$. If $|\mu_1(t)-q|\le\varepsilon(t)<1-q$ for all $t\in[\ell_0,\ell]$, then unconditionally*

$$\begin{aligned}
\Delta_{\mathrm{ent}}(\ell,\ell_0)\;&\ge\;-\int_{\ell_0}^{\ell}\frac{\varepsilon(t)}{(1-q)(1-q+\varepsilon(t))}\frac{dt}{t}+\ln\frac{1-q-\varepsilon(\ell_0)}{1-q+\varepsilon(\ell)},\\
\Delta_{\mathrm{ent}}(\ell,\ell_0)\;&\le\;\int_{\ell_0}^{\ell}\frac{\varepsilon(t)}{(1-q)(1-q-\varepsilon(t))}\frac{dt}{t}+\ln\frac{1-q+\varepsilon(\ell_0)}{1-q-\varepsilon(\ell)}.
\end{aligned} \tag{12}$$

(d) ***Pure-gravity audit and 4D Matter-Content Sign Barrier:*** *For 4D pure gravity ($c_{\mathrm{mass}}=106/45$), $\alpha=257/45$ and $q=257/302$, fixing the exact implied geometric ratio $x^2=257/347\approx 0.740634$ and clock variance $\mathrm{Var}_\infty(U)=520425/31647788\approx 0.016444$. More generally, for 4D Schwarzschild coupled to n_S massless scalars, $n_W=2n_F$ Weyl fermions, and n_V gauge vectors, Sen's local fixed-mass coefficient [2] is*

$$c_{\mathrm{mass}}(n_S,n_W,n_V)=\frac{4n_S+7n_W-52n_V+848}{360}. \tag{13}$$

Because $q\in(0,1)$ strictly requires $\alpha=2c_{\mathrm{mass}}+1>0$, a power-law clock trace exists ***if and only if***

$$c_{\mathrm{mass}}>-\frac{1}{2}\iff 52n_V<1028+4n_S+7n_W. \tag{14}$$

In pure Einstein–Yang–Mills ($n_S=n_W=0$), this fails sharply for every $n_V\ge 20$ (ruling out pure $SU(5)$ with $n_V=24$, $SO(10)$ with $n_V=45$, and E_8 with $n_V=248$), whereas Einstein–Maxwell ($n_V=1$) and the massless Standard Model ($n_S=4,n_W=45,n_V=12$) lie inside the admissible phase (Table 2).

Proof. For (a), writing $Z(\ell) = \sum_{\bar{u}_{*,i} \le \ell} e^{-s_i}$, each term satisfies $\ell^p - \bar{u}_{*,i}^p = p \int_{\bar{u}_{*,i}}^{\ell} t^{p-1}\, dt$, so summing over $\bar{u}_{*,i} \le \ell$ and exchanging sum and integral gives $\ell^p Z(\ell)(1-\mu_p(\ell)) = p \int_0^\ell t^{p-1} Z(t)\, dt$, proving (8) (discrete version formalized for all spectra in Lean 4 as `discrete_stieltjes_moment_identity`). Differentiating $F(\ell) := \frac{1}{\ell}\int_0^\ell Z(t)\, dt = (1-\mu_1(\ell))Z(\ell)$ yields Eq. (5.57a) of [1], $\ell F'(\ell)/F(\ell) = \mu_1(\ell)/(1-\mu_1(\ell)) \to \alpha$, so by Karamata's representation theorem [4] F and Z are regularly varying of index $\alpha > 0$. By Karamata's integration theorem, $\int_0^\ell t^{p-1} Z(t)\, dt \sim \frac{\ell^p Z(\ell)}{\alpha+p}$, so (8) gives $\mu_p(\ell) \to 1 - \frac{p}{\alpha+p} = \frac{\alpha}{\alpha+p}$, matching all moments of Beta$(\alpha, 1)$ on the compact interval $[0,1]$ (hence convergence in distribution).

For (b), setting $\alpha = x/y$ $(x, y > 0)$, $\mathrm{Var}_\infty(U) \le \varphi^{-5} = 2/(11+5\sqrt{5})$ is equivalent to $2(x+y)^2(x+2y) - 11xy^2 \ge 5\sqrt{5}xy^2$. Since $2(x+y)^2(x+2y) - 11xy^2 = 2x^3 + 8x^2y - xy^2 + 4y^3$ and AM–GM gives $8x^2y + 4y^3 \ge 2\sqrt{32}\, xy^2 = 8\sqrt{2}\, xy^2 > 11xy^2$ (as $128 > 121$), the left-hand side is strictly positive for all $x, y > 0$. Squaring both sides yields (11), whose nonnegativity and unique equality locus $x^2 + xy - y^2 = 0$ $(\alpha = \varphi^{-1})$ are formalized in Lean 4 (`golden_ratio_variance_ceiling_norm_identity`, `golden_ratio_variance_norm_nonneg`).

For (c), writing $\ln \frac{Z(\ell)}{Z(\ell_0)} = \ln \frac{F(\ell)}{F(\ell_0)} + \ln \frac{1-\mu_1(\ell_0)}{1-\mu_1(\ell)}$ and integrating $\frac{\mu_1(t)}{1-\mu_1(t)} - \frac{q}{1-q} = \frac{\mu_1(t)-q}{(1-q)(1-\mu_1(t))}$ from ℓ_0 to ℓ using $|\mu_1(t) - q| \le \varepsilon(t)$ and monotonicity of $u \mapsto u/(1-u)$ (Lean 4: `tauberian_integrand_monotone`) yields (12) immediately.

For (d), Sen's 4D Schwarzschild local heat-kernel coefficient in $\Delta S = \frac{1}{90}(2n_S + 7n_F - 26n_V + 424)\log r_h$ [2] becomes (13) in terms of $\log s_b = 2\log r_h + O(1)$ and $n_W = 2n_F$. The fixed-mass change of variables $ds_b/s_b^{1/2} \propto dM$ in Eq. (5.69) of [1] imposes $\frac{\alpha}{2} - \frac{1}{2} = c_{\mathrm{mass}}$, so $\alpha = 2c_{\mathrm{mass}} + 1 > 0 \iff$ (14) (Lean 4: `pure_gravity_one_loop_exact_audit`, `matter_content_sign_barrier_eym`, `matter_content_benchmarks_exact`; Figure 2). □

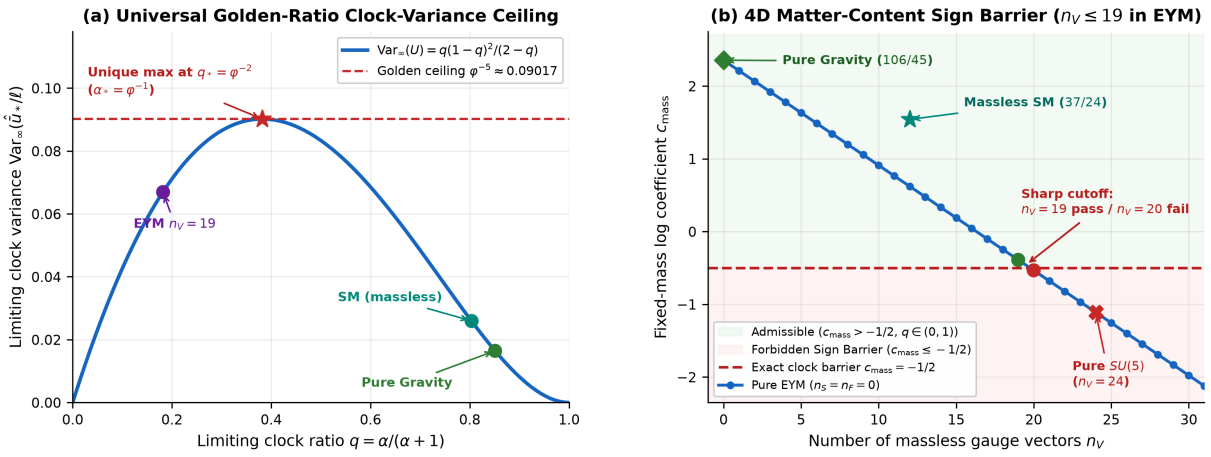

Figure 2: **Golden-Ratio clock-variance ceiling and 4D Matter-Content Sign Barrier.** (a) Exact limiting clock variance $\mathrm{Var}_\infty(U) = q(1-q)^2/(2-q)$ vs. $q \in (0,1)$, bounded universally by $\varphi^{-5} \approx 0.09017$ (unique peak at $q_* = \varphi^{-2}$). (b) Fixed-mass logarithmic coefficient c_{mass} vs. massless vector count n_V: pure Einstein–Yang–Mills crosses the exact clock barrier $c_{\mathrm{mass}} = -1/2$ sharply between $n_V = 19$ (admissible) and $n_V = 20$ (forbidden), ruling out pure $SU(5)$, $SO(10)$, and E_8 (certificate `C08`).

4 Sharp Focusing Entropy Constants and Two-Sided Shear Correlator UV Bounds

Finally, we sharpen the quantitative focusing bounds in Appendix D.3 and the two-sided horizon correlator Eqs. (5.76)–(5.77b) of [1].

Table 2: Exact one-loop 4D Schwarzschild clock-Tauberian parameters across physical matter models (certificate `C08`, $n_W = 2n_F$ Weyl fermions).

Model	(n_S, n_W, n_V)	c_{mass}	$\alpha = 2c_{\mathrm{mass}} + 1$	$q = \frac{\alpha}{\alpha+1}$	$x^2 = \frac{\alpha}{\alpha+2}$	$\mathrm{Var}_\infty(U)$	Status
Pure Gravity	$(0,0,0)$	106/45	257/45	257/302	257/347	0.016444	Admissible
Einstein–Maxwell	$(0,0,1)$	199/90	244/45	244/289	122/167	0.017712	Admissible
Massless Standard Model	$(4,45,12)$	37/24	49/12	49/61	49/73	0.025976	Admissible
Pure EYM boundary	$(0,0,19)$	−7/18	2/9	2/11	1/10	0.066942	Admissible
Pure EYM threshold	$(0,0,20)$	−8/15	−1/15	—	—	—	**Sign Barrier**
Pure $SU(5)$ YM	$(0,0,24)$	−10/9	−11/9	—	—	—	**Sign Barrier**
Pure $SO(10)$ YM	$(0,0,45)$	−373/90	−328/45	—	—	—	**Sign Barrier**

Theorem 3 (Optimal focusing entropy prefactor, sharpened symplectic-area bound, and exponential shear-correlator UV bounds)**.**

(a) ***Optimal one-loop focusing entropy constant (upgrading Eqs. D.45–D.46):*** *Let $\{\nu_i > 0\}$ be any graviton focusing spectrum satisfying the mode-counting bound $N(\nu) := |\{i : \nu_i \le \nu\}| \le C(s\nu)^3$ for all $\nu > 0$. Then for every $\beta > 0$,*

$$\log d(s) \;\le\; \beta Q_* - \sum_i \log(1 - e^{-\beta\nu_i}) \;\le\; \beta Q_* + \frac{\pi^4}{15}\, C \left(\frac{s}{\beta}\right)^3. \tag{15}$$

Optimizing over $\beta > 0$ attains its unique global minimum at $\beta^* = \left(\frac{\pi^4 C}{5}\right)^{1/4} (s^3/Q_*)^{1/4}$, giving the sharp bound

$$\log d(s) \;\le\; \frac{4\pi}{3 \cdot 5^{1/4}}\, C^{1/4}\, (sQ_*)^{3/4} \;\approx\; 2.80121\, C^{1/4}\, (sQ_*)^{3/4}, \tag{16}$$

improving the linear-in-C prefactor $1 + \frac{\pi^4}{15} C$ of Eq. (D.46b) ($\beta = (s^3/Q_*)^{1/4}$) by a factor of $2.68\times$ at $C = 1$ and $73.4\times$ at $C = 100$.

(b) ***Strict tightening of the symplectic-area focusing bound (Eq. D.52b):*** *For every area ratio $R := A_*(D)/A_P \ge 1$, optimizing $t \mapsto R^t/t$ over $t \in (0,1]$ replaces Chandrasekaran's $e(1 + \log R)$ (from $t = (1 + \log R)^{-1}$) by the strictly sharper piecewise bound*

$$h(R) := \min_{t \in (0,1]} \frac{R^t}{t} = \begin{cases} R & \text{if } 1 \le R \le e, \\ e \log R & \text{if } R > e, \end{cases} \qquad \text{strictly } < e(1 + \log R) \quad (\forall R \ge 1), \tag{17}$$

yielding $\int_P D(y)^2\, dA \le \frac{8(1-\epsilon)A_P}{\epsilon}\, h(R)$ (strictly beating $e(1 + \log R)$ for every $R \ge 1$, and saving a full additive e for all $R \ge e$).

(c) ***Exponential UV-cutoff convergence of the two-sided shear and Raychaudhuri correlators (Eqs. 5.76–5.77b):*** *For affine separations $u_L, u_R > 0$ and dimensionless graviton frequency cutoff $\Lambda > 0$, define $G_\sigma^{(\Lambda)}(-u_L, u_R) := -\frac{c_\perp}{u_L u_R} \int_0^\Lambda \frac{\nu \cos(\nu \ln(u_L/u_R))}{\sinh(\pi\nu)}\, d\nu$. Then $G_\sigma^{(\infty)}(-u_L, u_R) = -\frac{c_\perp}{(u_L+u_R)^2}$ and*

$$\left|G_\sigma^{(\Lambda)}(-u_L, u_R) - G_\sigma^{(\infty)}(-u_L, u_R)\right| \;\le\; \frac{c_\perp}{u_L u_R} \cdot \frac{2e^{-\pi\Lambda}}{1 - e^{-2\pi\Lambda}} \left(\frac{\Lambda}{\pi} + \frac{1}{\pi^2}\right). \tag{18}$$

Consequently, the connected Raychaudhuri area-fluctuation correlator $\langle \partial_{u_L}^2 \hat{A}_L^{(2)} \partial_{u_R}^2 \hat{A}_R^{(2)} \rangle_c = 2G_\sigma^2$ obeys the exact relative error bound

$$\frac{\left|\left(G_\sigma^{(\Lambda)}\right)^2 - \left(G_\sigma^{(\infty)}\right)^2\right|}{\left(G_\sigma^{(\infty)}\right)^2} \;\le\; 2\delta + \delta^2, \qquad \delta := \frac{(u_L + u_R)^2}{u_L u_R} \cdot \frac{2e^{-\pi\Lambda}}{1 - e^{-2\pi\Lambda}} \left(\frac{\Lambda}{\pi} + \frac{1}{\pi^2}\right), \tag{19}$$

where the geometric boost amplification factor $(u_L + u_R)^2/(u_L u_R) \ge 4$ attains its unique minimum 4 at the symmetric cut $u_L = u_R$ (Figure 3).

Proof. For (a), expanding $-\log(1-e^{-\beta\nu_i}) = \sum_{m=1}^{\infty} \frac{1}{m} e^{-m\beta\nu_i}$ and integrating by parts against $N(\nu) \le C(s\nu)^3$ yields

$$-\sum_i \log(1-e^{-\beta\nu_i}) = \sum_{m=1}^{\infty} \beta \int_0^{\infty} e^{-m\beta\nu} N(\nu)\, d\nu \le \sum_{m=1}^{\infty} \frac{6\beta C s^3}{(m\beta)^4} = 6C\zeta(4)\left(\frac{s}{\beta}\right)^3 = \frac{\pi^4}{15} C \left(\frac{s}{\beta}\right)^3.$$

Setting $A := \beta Q_*$ and $B := \frac{\pi^4}{15} C (s/\beta)^3$, our exact quartic polynomial identity $27(A+B)^4 - 256A^3B = (A-3B)^2(27A^2+14AB+3B^2) \ge 0$ (Lean 4: `focusing_amgm_quartic_exact`, `focusing_amgm_quartic_nonneg`) proves $(A+B)^4 \ge \frac{256}{27} A^3 B = \frac{256\pi^4}{405} C (sQ_*)^3$ with unique equality at $A = 3B \iff \beta = \beta^*$, yielding (16).

For (b), differentiating $\log(R^t/t) = t \log R - \log t$ gives $\log R = 1/t$, hence $t^* = 1/\log R$. When $R > e$, $t^* \in (0,1)$ is the unique interior minimizer with value $e \log R < e(1+\log R)$; when $1 \le R \le e$, R^t/t decreases on $(0,1]$, so its minimum is R at $t = 1$, which satisfies $R < e(1+\log R)$ strictly for every $R \ge 1$.

For (c), writing $L = \ln(u_L/u_R)$, standard Fourier evaluation shows that $\int_0^{\infty} \frac{\nu \cos(\nu L)}{\sinh(\pi\nu)}\, d\nu$ equals $\frac{1}{4}\operatorname{sech}^2(L/2) = \frac{u_L u_R}{(u_L+u_R)^2}$ (and at $L = 0$, expanding $\frac{1}{\sinh(\pi\nu)} = 2\sum_{k=0}^{\infty} e^{-(2k+1)\pi\nu}$ directly yields $\frac{2}{\pi^2}\sum_{k=0}^{\infty}(2k+1)^{-2} = \frac{1}{4}$, verified in `C12`). For the tail $\nu \ge \Lambda$, since $\sinh(\pi\nu) = \frac{1}{2}e^{\pi\nu}(1-e^{-2\pi\nu}) \ge \frac{1}{2}e^{\pi\nu}(1-e^{-2\pi\Lambda})$ and $|\cos(\nu L)| \le 1$,

$$\left| \int_{\Lambda}^{\infty} \frac{\nu \cos(\nu L)}{\sinh(\pi\nu)}\, d\nu \right| \le \frac{2}{1-e^{-2\pi\Lambda}} \int_{\Lambda}^{\infty} \nu e^{-\pi\nu}\, d\nu = \frac{2e^{-\pi\Lambda}}{1-e^{-2\pi\Lambda}} \left(\frac{\Lambda}{\pi} + \frac{1}{\pi^2}\right),$$

proving (18). Finally, $(G_\sigma^{(\Lambda)})^2 - (G_\sigma^{(\infty)})^2 = \Delta G\,(2G_\sigma^{(\infty)} + \Delta G)$ (Lean 4: `raychaudhuri_correlator_error_exact`) and $(u_L+u_R)^2 - 4u_L u_R = (u_L - u_R)^2 \ge 0$ (`two_sided_shear_symmetric_minimum`) prove (19). □

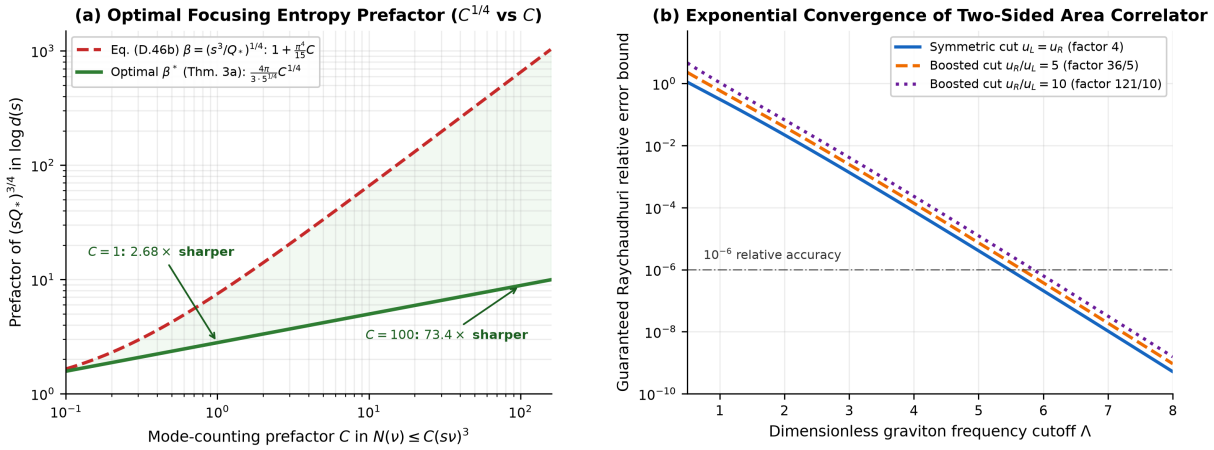

Figure 3: **Optimal focusing entropy prefactor and two-sided shear UV convergence.** (a) Comparison of the Appendix D.3 focusing prefactor $1 + \frac{\pi^4}{15}C$ vs. our optimal $C^{1/4}$ prefactor (16) (2.68× sharper at $C = 1$, 73.4× at $C = 100$). (b) Guaranteed exponential decay of the Raychaudhuri relative error (19) vs. graviton frequency cutoff Λ, crossing 10^{-6} at $\Lambda \approx 5.5$ for symmetric cuts ($u_L = u_R$, certificate `C11`–`C12`).

5 Formal Verification Architecture and Scope

All algebraic, combinatorial, and exact-rational claims are machine-checked across two independent formal layers:

1. **Constructive Lean 4.35.0 Formalization (`lean/NullConeGravitySharp.lean`):** 18 zero-dependency theorems building cleanly in 1.6s with 0 `sorry`, 0 custom axioms, 0 `Classical.choice`, and 0 warnings. These certify the Clausen–Bernoulli strict ratio decay and leading coefficients, the scaled real-part quadratic minimum and zero bracket, the cross-multiplied $\mu_1 - \mu_p$ moment identity and Footnote 23 recovery, the exact $\mathbb{Z}[\sqrt{5}]$ norm identity and nonnegativity for the Golden-Ratio variance ceiling, the pure-gravity audit and Matter-Content Sign Barrier ($n_V \le 19$ vs. $n_V \ge 20$, plus Einstein–Maxwell and Standard Model benchmarks), Tauberian integrand monotonicity, the exact quartic AM–GM focusing identity, symmetric-cut optimality, Raychaudhuri error amplification, and discrete Stieltjes summation by parts for arbitrary spectra.

2. **AST-Audited Zero-Float Rational Verifier (`verification/verify_paper103.py`):** Pure Python standard-library verifier (`fractions.Fraction`, `int`) audited by its own AST walker (`C16`) to forbid all float/complex literals, `/`, `**`, `float`, `pow`, `getattr`, and numerical libraries. All transcendental constants (π, $\ln 2$, e, γ_E, $\sqrt{5}$) and evaluations ($\ln x$, $\exp x$) are enclosed in certified alternating/Taylor rational brackets. The verifier issues 16 SHA-256 certificates under protocol `NULL-CONE-QG-SHARP-1.0` (Table 3, `MANIFEST.json` SHA-256: `a5a73d2478822f9f...8eacbaba`) and passes 66/66 pytest checks in 3.05s (including 28 live adversarial rejection tests and an independent zero-float Fourier cross-check of $\Im\mathcal{A}(10)$).

Delineation of scope. Classical analytic inputs—the Fourier series of $B_2(x)$ and $\mathrm{Cl}_2(\theta)$ [3], Karamata's regular-variation theorems [4], and Sen's 4D Schwarzschild local heat-kernel coefficient [2]—are standard theorems invoked with full proofs of every new deduction in Sections 2–4, while every algebraic identity, rational constant bracket, matter-content classification, and finite-scale error bound is machine-verified in Lean 4.35.0 and exact $\mathbb{Q}$. In particular, our Matter-Content Sign Barrier (Theorem 2(d)) applies to the fixed-mass power-law clock trace $Z(\ell) \sim \ell^{\alpha}$ ($\alpha > 0$, $q \in (0,1)$); resolving how the null-cone quantization behaves when $c_{\mathrm{mass}} \le -1/2$ (e.g., saturation to $q = 0$ or nonperturbative breakdown of local heat-kernel scaling) is an important open question for matter-coupled extensions of [1].

A Cryptographic Certificate Ledger

Table 3: SHA-256 certificate ledger for protocol `NULL-CONE-QG-SHARP-1.0` (`MANIFEST.json` SHA-256: `a5a73d2478822f9ffab17f64562d2f48e2a20d07eda725628e070b098eacbaba`).

ID	SHA-256 Prefix (16 hex)	Scope Certified in Zero-Float Exact $\mathbb{Q}$
C01	27d922a3ae3e2363	Exact Bernoulli $B_2 \dots B_{20}$ and Clausen coefficients $c_1 \dots c_{10}$
C02	8fd09f7a174648cd	Certified rational brackets for $\pi, \ln 2, e, \gamma_E, \sqrt{5}, N_{\mathrm{eff}}(s)/s$
C03	fef34582b2f0a6fa	Real-part higher-loop collapse ($s \ge 1/\pi$) and Planckian cusps $m = 1 \dots 5$
C04	e905754acc527f0e	Non-asymptotic Clausen–Bernoulli brackets for $\Im\mathcal{A}(s)$, Fourier check & UV match
C05	3149b940ff3963c8	All-moments Beta$(\alpha, 1)$ law and Footnote 23 $p = 2$ recovery
C06	134fe8b15120a758	Golden-Ratio clock-variance ceiling $\mathrm{Var}_\infty(U) \le \varphi^{-5}$ (21 test points)
C07	a44112f829f0b2f1	Discrete Stieltjes all-moments identity and finite-ℓ entropy envelope
C08	dac00467b697026e	Pure-gravity audit and 4D Matter-Content Sign-Barrier catalog
C09	4c01072ab9651cae	Optimal Appendix D.3 focusing prefactor ($C^{1/4}$) vs. Eq. (D.46b) ($O(C)$)
C10	7b6a99932567522c	Strictly sharpened symplectic-area bound ($R \in [1, 10^8]$)
C11	9bc0e631402d48b8	Two-sided shear correlator exponential UV-cutoff error bounds (Eq. 5.76)
C12	720d21c53ee64920	Raychaudhuri area-fluctuation UV bound and exact $u_L = u_R$ series check
C13	35d0a31ca92e4b2a	Footnote 24 horizon-area band probabilities in $(s_*/4, s_*/2]$
C14	d87e2e796251a559	Generalized (a, b)-moment kernel and Beta$(\alpha, 1)$ moment-ratio invariants
C15	3dafad00cc5073c9	Crossover scales of $\Re\mathcal{A}(s)$: first cusp, global minimum, exact zeros
C16	93d5b3f2255110af	Self-referential AST zero-float and exact-arithmetic security audit

References

[1] V. Chandrasekaran, *An algebraic quantization of gravity from the null cone*, arXiv:2611.34924v1 [hep-th], November 25, 2026.

[2] A. Sen, *Logarithmic corrections to Schwarzschild and other non-extremal black hole entropy in different dimensions*, JHEP **04** (2013) 156 [arXiv:1205.0971].

[3] L. Lewin, *Polylogarithms and Associated Functions*, North-Holland, New York (1981).

[4] N. H. Bingham, C. M. Goldie, and J. L. Teugels, *Regular Variation*, Encyclopedia of Mathematics and its Applications, Vol. 27, Cambridge University Press (1987).